Nonlinear Dyn
DOI 10.1007/s11071-016-2940-9

ORIGINAL PAPER

A new lattice hydrodynamic model considering the effects of bilateral gaps on vehicular traffic flow

Yongfu Li · Yu Song · Bin Yang · Taixiong Zheng · Huizong Feng · Yinguo Li

Received: 9 December 2015 / Accepted: 29 June 2016

Abstract This study proposes a new lattice hydrodynamic model considering the effects of bilateral gaps on a road without lane discipline. In particular, a lattice hydrodynamic model is proposed to capture the impacts from the lateral gaps of the right-side and left-side sites of the considered lattice sites. Linear stability analysis of the proposed model is performed using the perturbation method to obtain the stability condition. Nonlinear analysis of the proposed model is performed using the reductive perturbation method to derive the modified Korteweg–de Vries (mKdV) equation to characterize the density wave propagation. Results from numerical experiments illustrate that the smoothness and stability of the proposed model are improved compared with the model that considers the effect of unilateral gap. Also, the proposed model is able to more quickly dissipate the effect of perturbation occurring in the vehicular traffic flow.

Keywords Lattice hydrodynamic model · Bilateral gaps · Linear stability analysis · Nonlinear analysis

Y. Li (✉) · Y. Song · H. Feng · Y. Li
Chongqing Collaborative Innovation Center for Information Communication Technology, College of Automation, Chongqing University of Posts and Telecommunications, Chongqing 400065, China
e-mail: laf1212@163.com

B. Yang · T. Zheng
College of Advanced Manufacturing, Chongqing University of Posts and Telecommunications, Chongqing 400065, China

1 Introduction

Traffic flow modeling aims to capture and characterize the interactions in the vehicular traffic flow, which can date back to 1950s and receive much considerable attention recently. Traffic flow models can be classified as microscopic or macroscopic models [1–4]. Microscopic models generally use the microscopic variables, i.e., velocity, position, and acceleration, to capture local interactions between individual vehicles. Macroscopic models mainly adopt the collective variables, i.e., average speed, local density, and volume (flow), to describe traffic flow properties [5].

In the category of microscopic models, car-following (CF) models are used to describe the interactions with preceding vehicles in the same lane based on the idea that the behavior of the following vehicle depends on the stimuli from the preceding vehicles [3]. Following this research line, various CF models have proposed to explain the traffic phenomenon in the real word [6–13], such as the optimal velocity (OV) model [6], generalized force (GF) model [7], full velocity difference (FVD) model [8], multiple headway, velocity, and acceleration difference (MHVAD) model [9]. However, the above-mentioned CF models restrict the limitation to the assumption that vehicles follow the lane discipline and move in the middle of the lane. This assumption may not be valid in many developing countries where lanes may not be clearly demarcated on a road though multiple vehicles can travel in parallel [14–17]. To address this scenario, Jin

Published online: 11 July 2016

et al. [16] propose a non-lane-based full velocity difference CF (NLBCF) model to analyze the impact of the unilateral gap on the CF behavior. However, the NLBCF model cannot distinguish the right-side or the left-side later gaps. Consequently, Li et al. [17] propose a generalized model which considers the effects of two-sided lateral gaps of the following vehicle under non-lane-discipline-based environment. In addition, Li et al. [18] further study the effects of lateral gaps on the energy consumption for electric vehicle (EV) flow. Results from numerical experiments show that the characteristics in terms of lateral distribution of traffic flow may lead to different energy consumption in EV traffic flow. However, the aforementioned studies mainly rely on the OV-based traffic flow models, which belong to a microscopic viewpoint.

In the category of macroscopic models, lattice hydrodynamic models study the traffic behavior based on the assumption that the road can be divided into separate lattice sites [19–34]. Based on this assumption, Nagatani [19] proposes the first lattice hydrodynamic model based on the continuum model. Later, Nagatani [20] performs the nonlinear analysis of the lattice model to obtain the TDGL and mKdV equations. Li et al. [21] carry out the stability analysis of the lattice model considering the relative current of traffic flow. Zhu et al. [22] propose a generalized optimal current lattice model with a consideration of multi-interaction of the front lattice sites. Peng et al. [23,24] study the performance of lattice model considering the effects of the honk and driver's memory, respectively. Li et al. [5] study the lattice hydrodynamic model-based delay feedback control of vehicular traffic flow considering the effects of density change rate difference. Recently, to investigate the effect of lateral gap on vehicular traffic flow from the macroscopic viewpoint, Peng et al. [29] propose a non-lane-based (NLB) lattice model with the consideration of the lateral effects of the lane width. However, the NLB lattice model restrict the limitation to effect of unilateral gap. It does not distinguish the right-side or the left-side later gaps of the considered lattice sites. Hence, there is a research need to study the effects of bilateral gaps on vehicular traffic flow from a macroscopic viewpoint.

Motivated by the scenarios with bilateral gaps, the primary objective in this paper is to develop a new macroscopic lattice hydrodynamic model considering the effects of bilateral gaps on vehicular traffic flow under the non-lane-discipline-based road system. Theoretical analyses show that the Nagatani's model [19] and NLB lattice model [29] are special cases of the proposed model. The linear stability of the proposed model is analyzed using the perturbation method to obtain the stability condition. Theoretical and simulation analyses verify that the smoothness and stability the proposed model is improved compared to that of NLB lattice models under the same condition. The nonlinear analysis of the proposed model is performed using the reductive perturbation method to obtain the corresponding mKdV equation, which can describe the density wave propagation such that the traffic congestion pattern and its evolution can be better understood. Finally, the numerical experiments conducted in this study verify that the capability of perturbation rejection of the proposed model is improved compared to that of the NLB lattice model under the same condition.

The rest of this paper is organized as follows: Sect. 2 proposes a new lattice hydrodynamic model considering the effects of bilateral gaps. Section 3 performs the linear stability analysis of proposed model using the perturbation method. Section 4 conducts the nonlinear analysis using the reductive perturbation method. Section 5 conducts the numerical experiments and comparisons. The final section concludes this study.

2 Model derivation

In 1998, suppose the road is divided into N lattice sites, Nagatani [19] proposed the lattice hydrodynamic model based on the continuum models as follows:

$$\begin{aligned} &\partial_t \rho_j + \rho_0(\rho_j v_j - \rho_{j-1} v_{j-1}) = 0 \\ &\partial_t \rho_j v_j = a\rho_0 V(\rho_{j+1}) - a\rho_j v_j \end{aligned} \tag{1}$$

where j denotes the site j on the one-dimensional lattice, and $\rho_j(t)$ and $v_j(t)$ denote the local density and its corresponding local velocity on site j at time t, respectively. ρ_0 is the local average density, and $a = 1/\tau$ is the sensitivity of the driver. $V(\rho)$ represents the optimal speed of traffic flow at the density of ρ.

To address the scenario that all vehicles travel on a road without lane discipline, a new lattice hydrodynamic model considering the effects of bilateral gaps (BGL) as follows:

$$\rho_j(t+\tau) - \rho_j(t) + \tau\rho_0\left(\rho_j v_j - \rho_{j-1}v_{j-1}\right) = 0$$
$$\rho_j(t+\tau)v_j(t+\tau) = \rho_0 U\left(\rho_{j+1}, \rho_{j+2}, \rho_{j+3}\right) + \kappa G\left(\Delta Q_{j,j+1}, \Delta Q_{j,j+2}, \Delta Q_{j,j+3}\right) \quad (2)$$

where $\kappa \in \mathbb{R}$ is the reactive coefficient to the function $G(\cdot,\cdot,\cdot)$, $\Delta Q_{j,j+1} = \rho_{j+1}v_{j+1} - \rho_j v_j$ is the relative volume between site $j+1$ and j, $\Delta Q_{j,j+2} = \rho_{j+2}v_{j+2} - \rho_j v_j$ is the relative volume between site $j+2$ and j, $\Delta Q_{j,j+3} = \rho_{j+3}v_{j+3} - \rho_j v_j$ is the relative volume between site $j+3$ and j. In this scenario, lattice sites $j+1$ and $j+2$ position in right side and left side laterally in front of lattice site j, respectively. And lattice site $j+3$ positions in front of lattice site j.

Considering the bilateral gaps off the center line, the function $U(\cdot,\cdot,\cdot)$ and $G(\cdot,\cdot,\cdot)$ are defined as follows:

$$U\left[\rho_{j+1}, \rho_{j+2}, \rho_{j+3}\right] = \begin{cases} V[(1-2p_j)\rho_{j+1} + 2p_j\rho_{j+3}] \\ \quad Lg_{j,j+1} \in [0, 0.5Lg_{\max}] \\ V\left[(2p_j-1)\rho_{j+2} + 2(1-p_j)\rho_{j+3}\right] \\ \quad Lg_{j,j+1} \in [0.5Lg_{\max}, Lg_{\max}] \end{cases} \quad (3)$$

$$G\left[\Delta Q_{j,j+1}, \Delta Q_{j,j+2}, \Delta Q_{j,j+3}\right] = \begin{cases} (1-2p_j)\Delta Q_{j,j+1} + 2p_j\Delta Q_{j,j+3} \\ \quad Lg_{j,j+1} \in [0, 0.5Lg_{\max}] \\ (2p_j-1)\Delta Q_{j,j+2} + 2(1-p_j)\Delta Q_{j,j+3} \\ \quad Lg_{j,j+1} \in [0.5Lg_{\max}, Lg_{\max}] \end{cases} \quad (4)$$

$$V(\rho) = 0.5v_{\max}[\tanh(1/\rho - h_c) + \tanh(h_c)] \quad (5)$$

$$p_j = \frac{Lg_{j,j+1}}{Lg_{\max}} \quad (6)$$

where $V(\cdot)$ is the optimal speed, $v_{\max}$ is the maximal speed, h_c is the longitudinal safe space headway, and $\tanh(\cdot)$ is the hyperbolic tangent function [6]. $Lg_{j,j+1}$denotes the lateral gap between the site j and the right-side site $j+1$ and $Lg_{\max}$ is the lateral gap between the right-side site and the left-side site of site j. Then, the ratio $p_j \in [0,\ 1]$ indicates the relative location of site j with respect to the right-side site $j+1$ and the left-side site $j+2$.

Based on Eqs. (3)–(6), Eq. (2) can be reformulated as:

Case 1 if $Lg_{j,j+1} \in [0, 0.5Lg_{\max}]$

$$\rho_j(t+\tau) - \rho_j(t) + \tau\rho_0(\rho_j v_j - \rho_{j-1}v_{j-1}) = 0$$
$$\rho_j(t+\tau)v_j(t+\tau) = \rho_0 V\left[(1-2p_j)\rho_{j+1} + 2p_j\rho_{j+3}\right] + \kappa\left[(1-2p_j)\Delta Q_{j,j+1} + 2p_j\Delta Q_{j,j+3}\right] \quad (7)$$

Case 2 if $Lg_{j,j+1} \in [0.5Lg_{\max}, Lg_{\max}]$

$$\rho_j(t+\tau) - \rho_j(t) + \tau\rho_0(\rho_j v_j - \rho_{j-1}v_{j-1}) = 0$$
$$\rho_j(t+\tau)v_j(t+\tau) = \rho_0 V\left[(2p_j-1)\rho_{j+2} + 2(1-p_j)\rho_{j+3}\right] + \kappa\left[(2p_j-1)\Delta Q_{j,j+2} + 2(1-p_j)\Delta Q_{j,j+3}\right] \quad (8)$$

Remark 1 Equations (7) and (8) show that if the impact of lateral gaps on only one side is considered, the model is similar to the NLB lattice model in [29]; and if $Lg_{j,j+1} = 0$, $Lg_{j,j+1} = 0.5Lg_{\max}$, and $Lg_{j,j+1} = Lg_{\max}$, the model is deduced to the Nagatani's lattice model in [19]. Therefore, Nagatani's model and the NLB lattice model are some special cases of the proposed lattice model to some extent.

In addition, Eqs. (7) and (8) can be rewritten using the asymmetric forward difference as follows [17,29] to facilitate the stability analysis of the proposed lattice model as:

Case 1 if $Lg_{j,j+1} \in [0, 0.5Lg_{\max}]$

$$\rho_j(t+2\tau) - \rho_j(t+\tau) + \tau\rho_0^2\left\{V\left[(1-2p_j)\rho_{j+1} + 2p_j\rho_{j+3}\right] - V\left[(1-2p_j)\rho_j + 2p_j\rho_{j+2}\right]\right\} - \tau\kappa\left\{(1-2p_j)\left[\Delta\rho_{j,j+1}(t+\tau) - \Delta\rho_{j,j+1}(t)\right] + 2p_j\left[\Delta\rho_{j,j+3}(t+\tau) - \Delta\rho_{j,j+3}(t)\right]\right\} = 0 \quad (9)$$

Case 2 if $Lg_{j,j+1} \in [0.5Lg_{\max}, Lg_{\max}]$

$$\rho_j(t+2\tau) - \rho_j(t+\tau) + \tau\rho_0^2\{V[(2p_j-1)\rho_{j+2} + 2(1-p_j)\rho_{j+3}] - V[(2p_j-1)\rho_{j+1} + 2(1-p_j)\rho_{j+2}]\} - \tau\kappa\{(2p_j-1)[\Delta\rho_{j,j+2}(t+\tau) - \Delta\rho_{j,j+2}(t)] + 2(1-p_j)[\Delta\rho_{j,j+3}(t+\tau) - \Delta\rho_{j,j+3}(t)]\} = 0 \quad (10)$$

3 Linear stability analysis

The stability analysis of the proposed model is performed under the following assumption:

Assumption 1 The initial state of vehicular traffic flow is steady, and all vehicles in the traffic flow travel with the identical constant density and the optimal speed.

Based on the assumption, we conduct the stability analysis in terms of the two cases:

Case 1 if $Lg_{j,j+1} \in [0, 0.5Lg_{\max}]$

Following Assumption 1, the solution of the steady traffic flow is obtained as

$$\rho_j(t) = \rho_0, v_j(t) = V(\rho_0, \rho_0) \tag{11}$$

where $V(\rho_0, \rho_0) = V[(1-2p_j)\cdot\rho_0 + 2p_j\cdot\rho_0]$ is the optimal speed in uniform traffic flow and ρ_0 is the local average density.

Adding a small disturbance $y_j(t)$ to the steady-state flow solution, it follows that:

$$\rho_j(t) = \rho_0 + y_j(t) \tag{12}$$

Substituting Eq. (12) into Eq. (9) and linearizing the resulting equation using the Taylor expansion, it follows that

$$\begin{aligned} &y_j(t+2\tau) - y_j(t+\tau) + \tau\rho_0^2 V'(\rho_0,\rho_0) \\ &\quad\left[(1-2p_j)\Delta y_{j,j+1}(t) + 2p_j\Delta y_{j,j+3}(t)\right] \\ &\quad -\tau\kappa\left\{(1-2p_j)\left[\Delta y_{j,j+1}(t+\tau) - \Delta y_{j,j+1}(t)\right]\right. \\ &\quad \left.+2p_j\left[\Delta y_{j,j+3}(t+\tau) - \Delta y_{j,j+3}(t\right]\right\} = 0 \end{aligned} \tag{13}$$

where $\Delta y_{j,j+1}(t) = y_{j+1}(t) - y_j(t)$, $\Delta y_{j,j+3}(t) = y_{j+3}(t) - y_j(t)$. Set $y_j(t)$ be in the Fourier models, i.e., $y_j(t) = A\exp(\mathrm{ikj} + zt)$, substituting it into Eq. (13) and the resulting equation is:

$$\begin{aligned} &\mathrm{e}^{2\tau z} - \mathrm{e}^{\tau z} + \tau\rho_0^2 V'(\rho_0,\rho_0) \\ &\quad\times\left[(1-2p_j)\left(\mathrm{e}^{\mathrm{i}k} - 1\right) + 2p_j\left(\mathrm{e}^{3\mathrm{i}k} - 1\right)\right] \\ &\quad -\tau\kappa\left[(1-2p_j)(\mathrm{e}^{\tau z} - 1)\left(\mathrm{e}^{\mathrm{i}k} - 1\right)\right. \\ &\quad \left.+2p_j(\mathrm{e}^{\tau z} - 1)\left(\mathrm{e}^{3\mathrm{i}k} - 1\right)\right] = 0 \end{aligned} \tag{14}$$

Let $z = z_1(\mathrm{i}k) + z_2(\mathrm{i}k)^2 + \cdots$ and expand it to the second term of $(\mathrm{i}k)$ in Eq. (14), we obtain

$$\begin{aligned} &\left[1 + 2\tau z_1(ik) + \left(2\tau z_2 + 2\tau^2 z_1^2\right)(ik)^2\right] \\ &\quad -\left[1 + \tau z_1(ik) + \left(\tau z_2 + \frac{1}{2}\tau^2 z_1^2\right)(ik)^2\right] \\ &\quad +(1-2p_j)\tau\rho_0^2 V'(\rho_0,\rho_0) \\ &\quad\times\left(ik + \frac{1}{2}(ik)^2\right) + 2p_j\tau\rho_0^2 V'(\rho_0,\rho_0) \\ &\quad\times\left(3ik + \frac{9}{2}(ik)^2\right) - (1-2p_j)\tau^2\kappa z_1(ik)^2 \\ &\quad -6p_j\tau^2\kappa z_1(ik)^2 = 0 \end{aligned} \tag{15}$$

It follows from Eq. (15) that

$$\begin{cases} \tau z_1 = -\left[(1-2p_j)\tau\rho_0^2 V'(\rho_0,\rho_0)\right. \\ \qquad\left.+6p_j\tau\rho_0^2 V'(\rho_0,\rho_0)\right] \\ 2\tau z_2 + 2\tau^2 z_1^2 = \tau z_2 + \frac{1}{2}\tau^2 z_1^2 \\ \qquad -\frac{1}{2}(1-2p_j)\tau\rho_0^2 V'(\rho_0,\rho_0) \\ -9p_j\tau\rho_0^2 V'(\rho_0,\rho_0) + (1-2p_j)\tau^2\kappa z_1 + 6p_j\tau^2\kappa z_1 \end{cases} \tag{16}$$

Consequently,

$$\begin{cases} z_1 = -\rho_0^2 V'(\rho_0,\rho_0)(1+4p_j) \\ z_2 = -\left[\frac{1+8p_j}{2} + \tau(1+4p_j)\left(\kappa + \frac{3}{2}\rho_0^2 V'(\rho_0,\rho_0)\right)\right] \\ \qquad \rho_0^2 V'(\rho_0,\rho_0) \end{cases} \tag{17}$$

According to the long-wavelength method, when $z_1 > 0$ and $z_2 > 0$, the neutral stability condition is obtained as

$$\tau = -\frac{1+8p_j}{3\rho_0^2 V'(\rho_0,\rho_0) + 2\kappa(1+4p_j)} \tag{18}$$

Hence, for small disturbance with long wavelengths, the uniform traffic flow is unstable in the condition that

$$\tau > -\frac{1+8p_j}{3\rho_0^2 V'(\rho_0,\rho_0) + 2\kappa(1+4p_j)} \tag{19}$$

Case 2 if $Lg_{j,j+1} \in [0.5Lg_{\max}, Lg_{\max}]$

Using the similar method in case 1, the solution of the steady traffic flow is obtained as

$$\rho_j(t) = \rho_0, v_j(t) = V(\rho_0, \rho_0) \tag{20}$$

where $V(\rho_0, \rho_0) = V[(2p_j - 1)\cdot\rho_0 + 2(1-p_j)\cdot\rho_0]$ is the optimal velocity in uniform traffic flow. The neutral stability condition is obtained as

$$\tau = -\frac{7-4p_j}{3\rho_0^2 V'(\rho_0,\rho_0) + 2\kappa(4-2p_j)} \tag{21}$$

And the uniform traffic flow in this case is unstable when

$$\tau > -\frac{7-4p_j}{3\rho_0^2 V'(\rho_0,\rho_0)+2\kappa(4-2p_j)} \tag{22}$$

4 Nonlinear analysis

Following the reductive perturbation method [17,26,29], we analyze the nonlinear analysis of the proposed model to capture the jam formation. Starting from the definition of the small scaling parameters $\varepsilon(0<\varepsilon\ll 1)$ and new quantities have to be defined, i.e., the slow space, time variables X and T and perturbation R. To investigate the slowly varying behavior of slow scales near the critical point in the unstable region, the scaling between variables X and T and R are defined as follows [17,26,29]:

$$\begin{cases} X=\varepsilon(j+bt) \\ T=\varepsilon^3 t \\ \rho_j=\rho_c+\varepsilon R(X,T) \end{cases} \tag{23}$$

where b is an arbitrary constant that will be specified later.

Case 1 if $Lg_{j,j+1}\in[0,0.5Lg_{\max}]$
Based on the definition, substituting Eq. (23) into Eq. (9) and making the Taylor expansions to the fifth order of ε the resulting equation is:

$$\begin{aligned}&\varepsilon^2 k_1\partial_X R+\varepsilon^3 k_2\partial_X^2 R+\varepsilon^4\left(\partial_T R+k_3\partial_X^3 R+k_4\partial_X R^3\right)\\&\quad+\varepsilon^5\left(k_5\partial_T\partial_X R+k_6\partial_X^4 R+k_7\partial_X^2 R^3\right)=0\end{aligned} \tag{24}$$

The coefficients k_i $(i=1,2,\ldots,7)$ are given in Table 1.

Near the critical point (a_c,ρ_c), $\tau/\tau_c=1+\varepsilon^3$, $b=-\rho_0^2V'(\rho_0)$. Eliminating the second-order and third-order terms of ε in Eq. (24), it follows that:

$$\begin{aligned}&\varepsilon^4\left(\partial_T R+g_1\partial_X^3 R+g_2\partial_X R^3\right)\\&\quad+\varepsilon^5\left(g_3\partial_X^2 R+g_4\partial_X^4 R+g_5\partial_X^2 R^3\right)=0\end{aligned} \tag{25}$$

The coefficients g_i $(i=1,2,\ldots,5)$ are given in Table 2.

In order to obtain the standard mKdV equation for Eq. (25), the following transformations are introduced [17,26,29]:

$$T'=g_1T,\quad R=\sqrt{g_1/g_2}R' \tag{26}$$

Consequently, the regularized equation is referred

$$\partial_{T'}R'-\partial_{T'}^3R'+\partial_{T'}R'^3+\varepsilon M[R']=0 \tag{27}$$

Table 1 Coefficients k_i of the proposed model

k_1	k_2	k_3	k_4	k_5	k_6	k_7
$b+\rho_c^2V'$	$\frac{3}{2}b^2\tau+\frac{1}{2}\rho_c^2(1+8p_j)V'$	$\frac{7}{6}b^3\tau^2+\frac{1}{6}\rho_c^2V'(1+62p_j)$	$\rho_c^2\frac{1}{6}V'''$	$3b\tau$	$\frac{5}{8}b^4\tau^3+\frac{1}{24}\rho_c^2V'(1+14p_j)-$	$V'''\frac{1}{12}(1+2p_j)$
	$-kb(1+4p_j)$	$-\frac{kb}{2}[1+16p_j+b\tau(1+4p_j)]$			$\frac{kb}{12}[2(1+4p_j)b^2\tau^2+3(1+32p_j)b\tau+$	
					$2(1+52p_j)]$	

Table 2 Coefficients g_i of the proposed model

g_1	g_2	g_3	g_4	g_5
$-\frac{7}{6}b^3\tau^2-\frac{1}{6}\rho_c^2V'(1+62p_j)$ $+\frac{kb}{2}[1+16p_j+b\tau(1+4p_j)]$	$\frac{\rho_c^2V'''}{6}$	$\frac{3}{2}b^2\tau$	$-\frac{23}{8}b^4\tau^3+\frac{\rho_c^2V'}{24}(1+14p_j)$ $-\frac{b\tau\rho_c^2V'}{2}(1+62p_j)+\frac{3b^2\tau^2k[1+16p_j+b\tau(1+4p_j)]}{2}$ $-\frac{kb\tau}{12}[2(1+4p_j)b^2\tau^2+3(1+32p_j)b\tau+2(1+52p_j)]$	$V'''\frac{1}{12}[(1+2p_j)-$ $6b\tau]$

Table 3 Coefficients β_i of the proposed model

β_1	β_2	β_3	β_4	β_5	β_6	β_7
$b+\rho_c^2V'$	$\frac{3}{2}b^2\tau+$ $\frac{1}{2}\rho_c^2(7-4p_j)V'$ $-kb(4-2p_j)$	$\frac{7}{6}b^3\tau^2+\frac{1}{6}\rho_c^2V'$ $(31-24p_j)$ $-kb[b\tau(2-p_j)+$ $(7-5p_j)]$	$\rho_c^2\frac{1}{6}V''''$	$3b\tau$	$\frac{5}{8}b^4\tau^3+\frac{1}{24}\rho_c^2V'$ $(115-100p_j)$ $-\frac{kb}{6}[b^2\tau^2(4-2p_j)+$ $b\tau(21-15p_j)$ $+(69-57p_j)]$	$V''''\frac{1}{12}(7-4p_j)$

where

$$M[R']=\frac{1}{g_1}\left(g_3\partial_X^2R'+\frac{g_1g_5}{g_2}\partial_X^2R'^3+g_4\partial_X^4R'\right) \tag{28}$$

Ignoring the $O(\varepsilon)$ term in Eq. (27), we obtain the mKdV equation with the kink–antikink solution

$$R_0'(X,T')=\left|\sqrt{c}\tanh\left[\sqrt{\frac{c}{2}}(X-cT')\right]\right| \tag{29}$$

Suppose $R'(X,T')=R_0'(X,T')+\varepsilon R_1'(X,T')$. In order to determine the selected value of the propagation velocity for the kink–antikink solution, it is necessary to satisfy the following condition [17,26,29]:

$$(R_0',M[R_0'])\equiv\int_{-\infty}^{+\infty}\mathrm{d}XR_0'M[R_0']=0 \tag{30}$$

where $M[R_0']=M[R']$. By solving Eq. (29), we obtain

$$c=5g_2g_3/(2g_2g_4-3g_1g_5) \tag{31}$$

Thus, the following kink–antikink soliton solution $(-\rho_c^2V'(\rho_c)=1,-\rho_c^6V'''(\rho_c)=2)$ of the mKdV equation is obtained by

$$\rho_j(t)=\rho_c+\sqrt{\frac{g_1c}{g_2}\left(\frac{\tau}{\tau_c}-1\right)}\tanh\sqrt{\frac{c}{2}\left(\frac{\tau}{\tau_c}-1\right)}\times\left[j+\left(1-cg_1\left(\frac{\tau}{\tau_c}-1\right)\right)t\right] \tag{32}$$

The amplitude A of the solution is given by

$$A=\sqrt{\frac{g_1c}{g_2}\left(\frac{\tau}{\tau_c}-1\right)} \tag{33}$$

Case 2 if $Lg_{j,j+1}\in[0.5Lg_{\max},Lg_{\max}]$

Similarly, substituting Eq. (23) into Eq. (10) and making the Taylor expansions to the fifth order of ε, the resulting equation is:

$$\varepsilon^2\beta_1\partial_XR+\varepsilon^3\beta_2\partial_X^2R+\varepsilon^4\left(\partial_TR+\beta_3\partial_X^3R+k_4\beta_XR^3\right)+\varepsilon^5\left(\beta_5\partial_T\partial_XR+\beta_6\partial_X^4R+\beta_7\partial_X^2R^3\right)=0 \tag{34}$$

The coefficients β_i $(i=1,2,\ldots,7)$ are given in Table 3.

Eliminating the second-order and third-order terms of ε in Eq. (34) near the critical point, it follows that:

$$\varepsilon^4(\partial_TR+\gamma_1\partial_X^3R+\gamma_2\partial_XR^3)+\varepsilon^5(\gamma_3\partial_X^2R+\gamma_4\partial_X^4R+\gamma_5\partial_X^2R^3)=0 \tag{35}$$

The coefficients γ_i $(i=1,2,\ldots,5)$ are given in Table 4.

In order to obtain the standard mKdV equation for Eq. (35), the following transformations are introduced [17,26,29]:

$$T'=\gamma_1T,\quad R=\sqrt{\gamma_1/\gamma_2}R' \tag{36}$$

Table 4 Coefficients γ_i of the proposed model

γ_1	γ_2	γ_3	γ_4	γ_5
$\frac{7}{6}b^3\tau^2 + \frac{1}{6}\rho_c^2 V'(31-24p_j)$ $-kb[b\tau(2-p_j)+(7-5p_j)]$	$\rho_c^2\frac{1}{6}V'''$	$\frac{3}{2}b^2\tau$	$-\frac{23}{8}b^4\tau^3 + \frac{1}{24}\rho_c^2 V'(115-100p_j) - \frac{\rho_c^2 V' b\tau}{2}(31-24p_j)$ $+3kb^2\tau[b\tau(2-p_j)+(7-5p_j)]$ $-\frac{kb}{6}[b^2\tau^2(4-2p_j)+b\tau(21-15p_j)+(69-57p_j)]$	$V'''\frac{1}{12}[(7-4p_j)-6b\tau]$

Consequently, the regularized equation is referred

$$\partial_{T'}R' - \partial^3_{T'}R' + \partial_{T'}R'^3 + \varepsilon M[R'] = 0 \tag{37}$$

where

$$M[R'] = \frac{1}{\gamma_1}\left(\gamma_3\partial^2_X R' + \frac{\gamma_1\gamma_5}{\gamma_2}\partial^2_X R'^3 + \gamma_4\partial^4_X R'\right) \tag{38}$$

Ignoring the $O(\varepsilon)$ term in Eq. (37), we obtain the mKdV equation with the kink–antikink solution

$$R'_0(X,T') = \left|\sqrt{c}\tanh\left[\sqrt{\frac{c}{2}(X-cT')}\right]\right| \tag{39}$$

Suppose $R'(X,T') = R'_0(X,T') + \varepsilon R'_1(X,T')$, in order to determine the selected value of the propagation velocity for the kink–antikink solution, it is necessary to satisfy the following condition [17,26,29]:

$$(R'_0, M[R'_0]) \equiv \int_{-\infty}^{+\infty} \mathrm{d}X R'_0 M[R'_0] = 0 \tag{40}$$

where $M[R'_0] = M[R']$. By solving Eq. (39), we obtain

$$c = 5\gamma_2\gamma_3/(2\gamma_2\gamma_4 - 3\gamma_1\gamma_5) \tag{41}$$

Thus, the following kink–antikink soliton solution ($-\rho_c^2 V'(\rho_c) = 1, -\rho_c^6 V'''(\rho_c) = 2$) of the mKdV equation is obtained by

$$\rho_j(t) = \rho_c + \sqrt{\frac{\gamma_1 c}{\gamma_2}\left(\frac{\tau}{\tau_c}-1\right)}\tanh\sqrt{\frac{c}{2}\left(\frac{\tau}{\tau_c}-1\right)} \times\left[j + \left(1 - c\gamma_1\left(\frac{\tau}{\tau_c}-1\right)\right)t\right] \tag{42}$$

The amplitude A of the solution is given by

$$.A = \sqrt{\frac{\gamma_1 c}{\gamma_2}\left(\frac{\tau}{\tau_c}-1\right)}. \tag{43}$$

5 Numerical experiments

Based on the foregoing theoretical analysis, numerical experiments are performed to verify the proposed model described in Eqs. (7) and (8) and demonstrate the dynamic performance. Suppose that there are N lattice sites on a road under a periodic boundary condition and the lateral gap is constant for all sites. The initial conditions are set as follows [29]:

$$\begin{aligned}&\rho_j(0) = \rho_0 = 0.25,\ \rho_j(1) = \rho_j(0) = 0.25 \quad \text{for} \quad j \neq 50, 51\\ &\rho_j(1) = \rho_j(0) = 0.25 - 0.1, \quad \text{for} \quad j = 50\end{aligned} \tag{44}$$

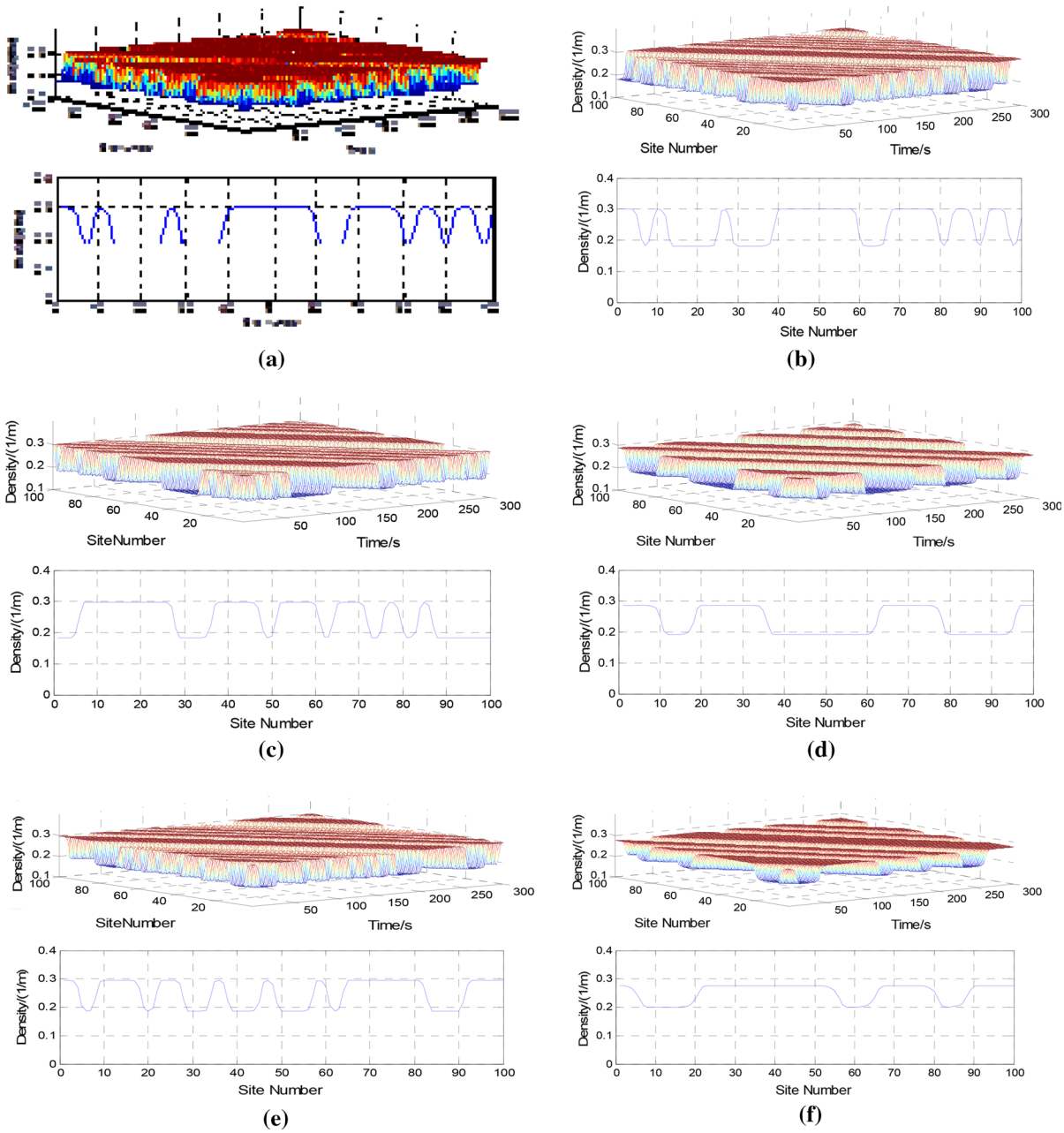

Fig. 1 Density wave after 10^4 time steps and the profile at $t = 10^4$, where **a**, **c**, **e**, **g**, **i** are the outputs from the unilateral gap condition while **b**, **d**, **f**, **h**, **j** are the outputs from the bilateral gaps condition with $p_j = 0, 0.01, 0.02, 0.03, 0.1$, respectively

$$\rho_j(1) = \rho_j(0) = 0.25 + 0.1, \quad \text{for} \quad j = 51 \tag{45}$$

In addition, other parameters are set as: $N = 100, h_c = 4\,\text{m}, \rho_c = 1/h_c, a = 2.0, k = 2.0$.

Figure 1 shows kink–antikink density profile after 10^4 time steps and the corresponding profile at the time step $t = 10^4$ The curves in Fig. 1 are the profiles of corresponding three-dimensional diagrams at the time step $t = 10^4$.

In Fig. 1, the parameter p_j is set as 0, 0.01, 0.02, 0.03 and 0.1. The subfigures on the left-hand side of Fig. 1, i.e., Fig. 1a, c, e, g, i, are the simulation results based on the NLB lattice model considering the effects

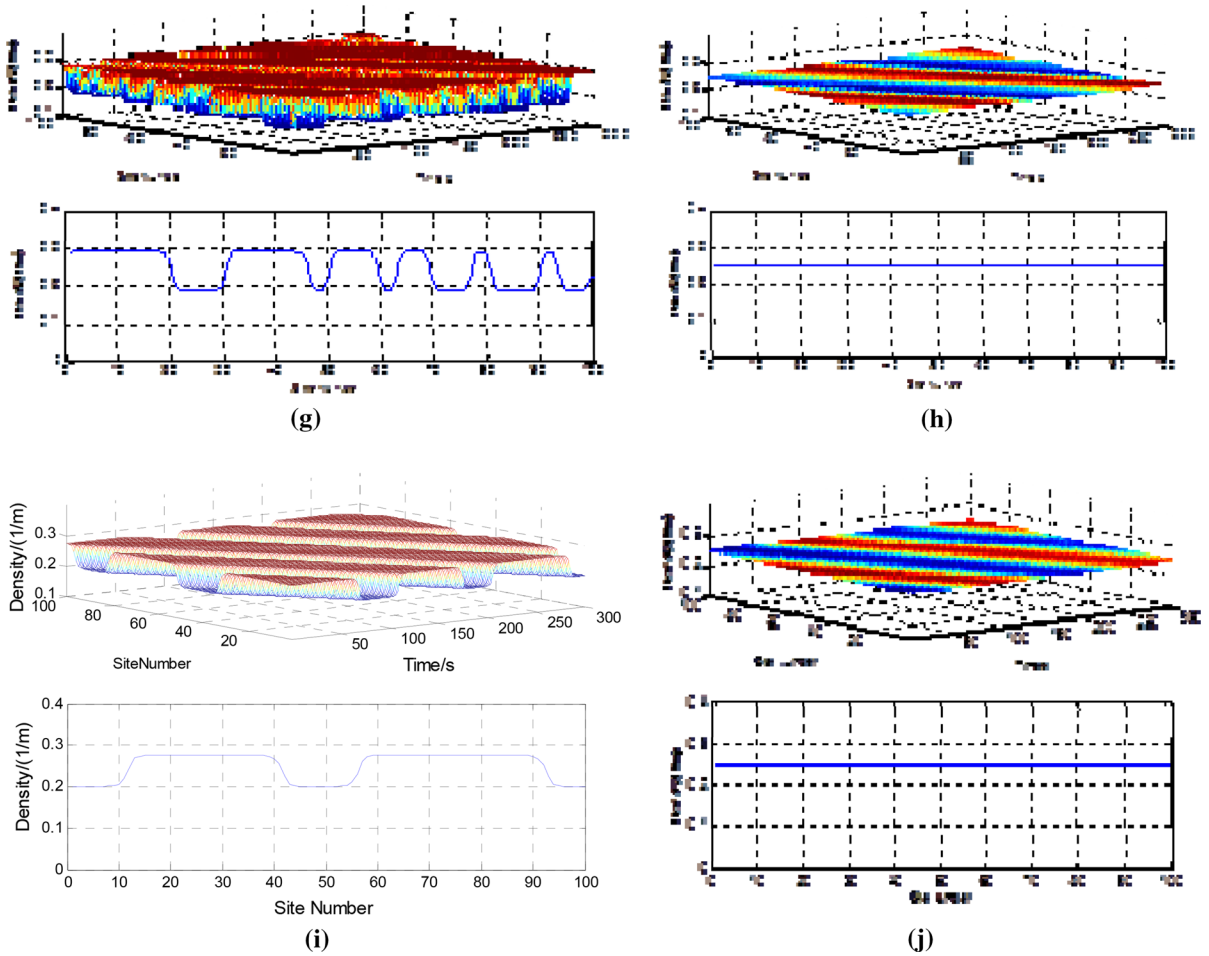

Fig. 1 continued

of unilateral gap in [29]. The subfigures on the right-hand side of Fig. 1, i.e., Fig. 1b, d, f, h are the simulation results based on the proposed model considering the effects of bilateral gaps. The comparisons are mainly to demonstrate the capability of perturbation rejection in the vehicular traffic flow. By comparing the results under unilateral gap and bilateral gaps conditions, the main findings are summarized as follows:

(i) Under the unilateral gap condition, as shown in Fig. 1a, c, e, g, i, the stop-and-go traffic appears with parameter p_j= 0, 0.01, 0.02, 0.03, 0.1, while the stop-and-go traffic disappears with parameter p_j = 0.03 under the bilateral gaps condition as shown in Fig. 1b, d, f, h, j. This accounts for the condition that when small perturbations in Eqs. (44) and (45) are put into the uniform traffic flow, they will be amplified with time and the uniform flow will eventually evolve toward a heterogeneous flow. The jams in Fig. 1a, b are the most serious in the NLB lattice model [29] and the proposed model, where there are no effects of lateral gaps. And when the effects of lateral gaps are considered, the smoothness and stability of traffic flow can be improved. As shown in Fig. 1c, e, and d, f, the amplitudes of perturbations decrease with the increase of p_j, and the traffic flow can evolve toward a homogeneous flow in NLB lattice model with $p_j = 0.3$ [29] and in the proposed model with $p_j = 0.03$.

(ii) Figure 1f–j indicates that the effects of bilateral gaps can improve the smoothness and stability of traffic flow. The introduction of effects of the bilateral gaps is necessary in traffic flow.

(iii) According to Fig. 1e, f, the dynamic performance of the proposed model is better than that of NLB lattice model [29]. That is to say traffic flow described by the proposed model can overcome the effects of small perturbations such as the sudden traffic event occurring in traffic flow with smaller value of parameter p_j than that of NLB lattice model. This is because the NLB lattice model only considers the effect of unilateral gap while the proposed model considers the effects of bilateral gap, which implies that the rich information of surrounding vehicles can enhance the performance of lattice model.

6 Conclusions

This study focuses on the macroscopic model of traffic flow under the non-lane-discipline-based road system. Considering the effects of bilateral gaps on traffic flow, a new lattice hydrodynamic model is proposed. Theoretical analysis proves that the Nagatani's lattice model and the NLB lattice model with unilateral gap are special cases of the proposed model. Stability condition of the proposed model is obtained through linear stability analysis using the perturbation method. The corresponding mKdV equation of the proposed model is derived through nonlinear analysis using the reductive perturbation method to describe the density wave propagation. In addition, results from simulation-based numerical experiments show that the proposed mode is able to more rapidly dissipate the effect of a perturbation occurring in traffic flow.

The findings of the study illustrate the effects of lateral gaps on traffic flow with respect to the smoothness and stability. Also, it motivate us to study the impacts of lateral gaps on the vehicular formation under non-lane-discipline-based road system in the future.

Acknowledgments Thanks to the support from the project by the National Natural Science Foundation of China (Grant No. 61304197), the Scientific and Technological Talents of Chongqing (Grant No. cstc2014kjrc-qnrc30002), the Key Project of Application and Development of Chongqing (Grant No. cstc2014yykfB40001), Wenfeng Talents of Chongqing University of Posts and Telecommunications, "151" Science and Technology Major Project of Chongqing-General Design and Innovative Capability of Full Information Based Traffic Guidance and Control System (Grant No. cstc2013jcsf-zdzxqqX0003), National Key Research and Development Program (2016YFB0100900), and the Doctoral Start-up Funds of Chongqing University of Posts and Telecommunication (Grant No. A2012-26).

References

1. Brackstone, M., McDonald, M.: Car-following: a historical review. Transp. Res. Part F **2**(4), 181–196 (1999)
2. Wilson, R.E., Ward, J.A.: Car-following models: fifty years of linear stability analysis—a mathematical perspective. Transp. Plan. Technol. **34**(1), 3–18 (2010)
3. Li, Y., Sun, D.: Microscopic car-following model for the traffic flow: the state of the art. J. Control Theory Appl. **10**(2), 133–143 (2012)
4. Saifuzzaman, M., Zheng, Z.: Incorporating human-factors in car-following models: a review of recent developments and research needs. Transp. Res. Part C **48**, 379–403 (2014)
5. Li, Y., Zhang, L., Zheng, T., Li, Y.: Lattice hydrodynamic model based delay feedback control of vehicular traffic flow considering the effects of density change rate difference. Commun. Nonlinear Sci. Numer. Simul. **29**(1–3), 224–232 (2015)
6. Bando, M., Hasebe, K., Nakayama, A., Shibata, A., Sugiyama, Y.: Dynamics model of traffic congestion and numerical simulation. Phys. Rev. E **1**(51), 1035–1042 (1995)
7. Helbing, D., Tilch, B.: Generalized force model of traffic dynamics. Phys. Rev. E **58**, 133–138 (1998)
8. Jiang, R., Wu, Q.S., Zhu, Z.J.: Full velocity difference model for a car-following theory. Phys. Rev. E **64**, 017101–017105 (2001)
9. Li, Y., Sun, D., Liu, W., Zhang, M., Zhao, M., Liao, X., Tang, L.: Modeling and simulation for microscopic traffic flow based on multiple headway, velocity and acceleration difference. Nonlinear Dyn. **66**(1–2), 15–28 (2011)
10. Tian, J., Jia, B., Li, X., Gao, Z.: A new car-following model considering velocity anticipation. Chin. Phys. B **19**(1), 010511–010519 (2010)
11. Tang, T., Wang, Y., Yang, X., Wu, Y.: A new car-following model accounting for varying road condition. Nonlinear Dyn. **70**(2), 1397–1405 (2012)
12. Li, Y., Zhu, H., Cen, M., Li, Y., Li, R., Sun, D.: On the stability analysis of microscopic traffic car-following model: a case study. Nonlinear Dyn. **74**(1–2), 335–343 (2013)
13. Tang, T., Shi, W., Shang, H., Wang, Y.: A new car-following model with consideration of inter-vehicle communication. Nonlinear Dyn. **76**(4), 2017–2023 (2014)
14. Chandra, S., Kumar, U.: Effect of lane width on capacity under mixed traffic conditions in India. J. Transp. Eng. **129**(2), 155–160 (2003)
15. Gunay, B.: Car following theory with lateral discomfort. Transp. Res. Part B **41**(7), 722–735 (2007)
16. Jin, S., Wang, D., Tao, P., Li, P.: Non-lane-based full velocity difference car following model. Phys. A **389**(21), 4654–4662 (2010)
17. Li, Y., Zhang, L., Peeta, S., Pan, H., Zheng, T., Li, Y., He, X.: Non-lane-discipline-based car-following model considering the effects of two-sided lateral gaps. Nonlinear Dyn. **80**(1–2), 227–238 (2015)
18. Li, Y., Zhang, L., Zheng, H., He, X., Peeta, S., Zheng, T., Li, Y.: Evaluating the energy consumption of electric vehi-

cles based on car-following model under non-lane discipline. Nonlinear Dyn. **82**(1), 1–13 (2015)
19. Nagatani, T.: Modified Kdv equation for jamming transition in the continuum models of traffic. Phys. A **261**, 599–607 (1998)
20. Nagatani, T.: TDGL and MKdV equations for jamming transition in the lattice models of traffic. Phys. A **264**(3), 581–592 (1999)
21. Li, Z., Li, X., Liu, F.: Stabilization analysis and modified KdV equation of lattice models with consideration of relative current. Int. J. Mod. Phys. C **19**(08), 1163–1173 (2008)
22. Zhu, W.X., Chi, E.X.: Analysis of generalized optimal current lattice model for traffic flow. Int. J. Mod. Phys. C **19**(05), 727–739 (2008)
23. Peng, G., Cai, X., Liu, C., Cao, B.: A new lattice model of traffic flow with the consideration of the honk effect. Int. J. Mod. Phys. C **22**(09), 967–976 (2011)
24. Peng, G.: A new lattice model of traffic flow with the consideration of individual difference of anticipation driving behavior. Commun. Nonlinear Sci. Numer. Simul. **18**(10), 2801–2806 (2013)
25. Ge, H.X., Cheng, R.J., Lei, L.: The theoretical analysis of the lattice hydrodynamic models for traffic flow theory. Phys. A **389**(14), 2825–2834 (2010)
26. Wang, T., Gao, Z., Zhao, X., Tian, J., Zhang, W.: Flow difference effect in the two-lane lattice hydrodynamic model. Chin. Phys. B **21**, 070507–070516 (2012)
27. Ge, H., Cui, Y., Zhu, K., Cheng, R.: The control method for the lattice hydrodynamic model. Commun. Nonlinear Sci. Numer. Simul. **22**(1), 903–908 (2015)
28. Li, Z., Zhang, R., Xu, S., Qian, Y.: Study on the effects of driver's lane-changing aggressiveness on traffic stability from an extended two-lane lattice model. Commun. Nonlinear Sci. Numer. Simul. **24**(1), 52–63 (2015)
29. Peng, G., Cai, X., Cao, B., Liu, C.: Non-lane-based lattice hydrodynamic model of traffic flow considering the lateral effects of the lane width. Phys. Lett. A **375**(30), 2823–2827 (2011)
30. Peng, G., Nie, F., Cao, B.: A driver's memory lattice model of traffic flow and its numerical simulation. Nonlinear Dyn. **67**(3), 1811–1815 (2012)
31. Ge, H., Zheng, P., Lo, S., Cheng, R.: TDGL equation in lattice hydrodynamic model considering driver's physical delay. Nonlinear Dyn. **76**(1), 441–445 (2014)
32. Wang, T., Gao, Z., Zhang, J.: Stabilization effect of multiple density difference in the lattice hydrodynamic model. Nonlinear Dyn. **73**(4), 2197–2205 (2013)
33. Gupta, A.K., Redhu, P.: Analyses of the driver's anticipation effect in a new lattice hydrodynamic traffic flow model with passing. Nonlinear Dyn. **76**(2), 27–34 (2014)
34. Gupta, A.K., Sharma, S., Redhu, P.: Effect of multi-phase optimal velocity function on jamming transition in a lattice hydrodynamic model with passing. Nonlinear Dyn. **80**(3), 1091–1108 (2015)